VIRTUAL FLIGHT THROUGH GLIAL CELLS

Mr J Meyer, Prof Dr H Hagen
Mr C Lohr, Prof Dr J W Deitmer
Univ. Kaiserslautern, Germany 98ME067

Abstract

Glial cells, as an important part of the brain and nervous system, implement voltage and ligand-gated membrane channels. Similar to neurons, macroglial cells comprise neurotransmitter receptors and ion-selective membrane channels. Leech giant glial cells are used to exemplify structural and physiological properties of this cell type.

In conjunction with confocal laser microscopy, three-dimensional scans can be obtained from a set of two-dimensional slices. Each virtual slice is represented by a designated focal plane. By shifting the focal plane, a 3-D stack of cross sections is conceived. The microscope enables views only from the top, or accumulated aspects through the object. A view from aside is not possible without rotating the object itself. This would require to remove the exiguous cell from the object slide, which would certainly destroy it.

Even so, arbitrary views should be enabled by the imaging system in order to reveal the entire structure of the microscopic object. In a lab environment, interactive exploration of the cell is required in order to study the nested structure and physical response while the cell is still alive (in-vivo study). Therefore, we have extended our InVIS (Interactive Visualization) system, which was originally designed for medical applications (CT or MRI), to confocal microscopy. We describe the structure of our system and new filtering techniques which have been added.

Introduction

The nervous systems of all animals, from coelenterates to chordates, contain two cell types, neurons and glial cells. Glial cells have been shown to maintain neuronal functions by providing neurons with nutrients, maintaining the ionic environment and guiding neurons during development [11].

In nervous systems of many invertebrates, like the leech, only a few glial cells form a ganglion with hundreds or thousands of neurons. Each segmental ganglion of the leech consists of the peripheral cell bodies of approximately 400 neurons and the central neuropile. The neuropile comprises neuronal cell processes that form synaptic contacts and two giant glial cells [1]. The latter possess large cell bodies with diameters of about 90 µm, which simplifies the identification of the cells and the performance of experiments.

The glial cells build intensely ramified arborizations that extend into the synaptic regions [3]. In recent studies, it has been shown that the giant glial cells of the leech can respond to neurotransmitters released from synaptic terminals with changes in their functional properties, which may affect physiological processes in neurons [9][10]. Figure 1 gives an example of a giant glial cell from a leech.

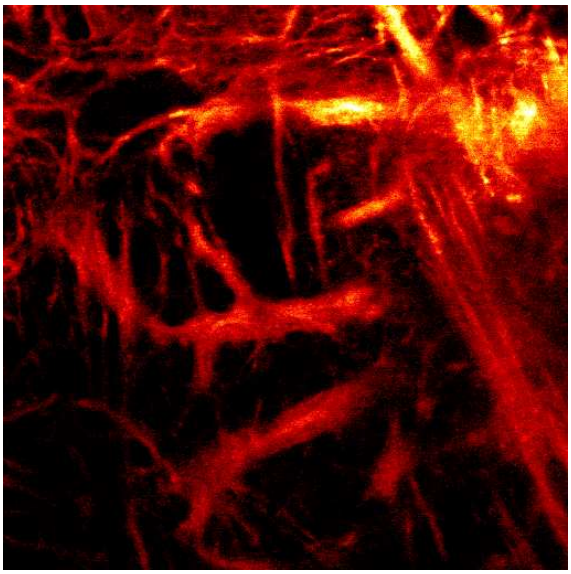

Fig. 1: giant glial cell

The three-dimensional structure of the glial cells and the morphological relationship between the glial cells and neuronal structures within the nervous system of the leech is of particular interest for interpreting these neuron-glia interactions.

Principle of Confocal Imaging

A confocal microscope uses a laser beam in conjunction with optical devices to scan small objects in three dimensions. Depth information is obtained by varying the focal plane of the laser beam. In this way, a series of two-dimensional slices can be created, where each slice represents a coplanar cross-section of the object (figures 2, 3).

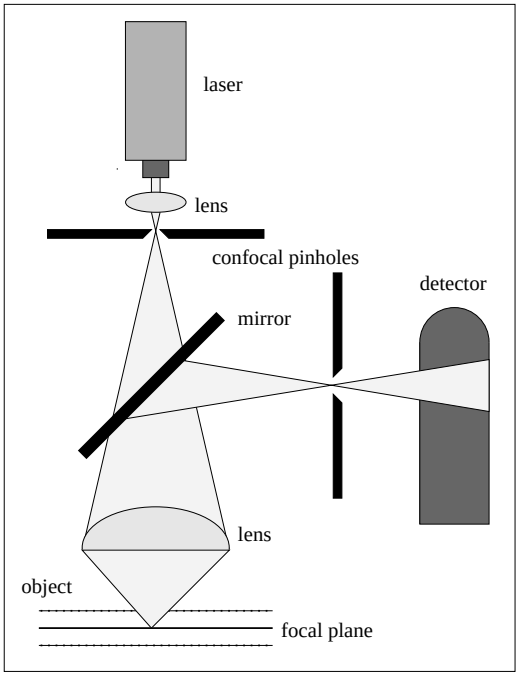

Fig. 2: principle of confocal imaging

The ray traverses a lens, which expands the laser beam, and a confocal pinhole, which is used to reduce stray light. A convex lens focusses the beam onto the object in a certain focal plain. A semi-transparent mirror reflects the light, which is emitted from the object, through the lens and through a second confocal pinhole into the detector. Scanning the object in *x* / *y*-direction as well as in *z*-direction (along the optical axis) allows for data acquisition in three dimensions.

One of the major improvements offered by a confocal microscope over the performance of a conventional microscope is the fact that light rays from outside the focal plane are almost eliminated. Due to the small dimension of the illuminating light spot in the focal plane, stray light is minimized.

Nevertheless, each slice from an image series contains fuzzy information from neighboring slices. Besides the wavelength of light, this effect depends in particular on the numerical aperture of the objective used and the diameter of the focal pinhole. A wider detection pinhole reduces the confocal effect.

By means of image processing, this blurring effect can be reduced by the application of filtering techniques. Contrary, image processing can also be used to superimpose several slices, giving an extended focus image which can only be achieved in conventional microscopy by reduction of the aperture and thus sacrificing resolution.

The next chapter explains the special filtering techniques that we applied in order to enhance the original data set before rendering.

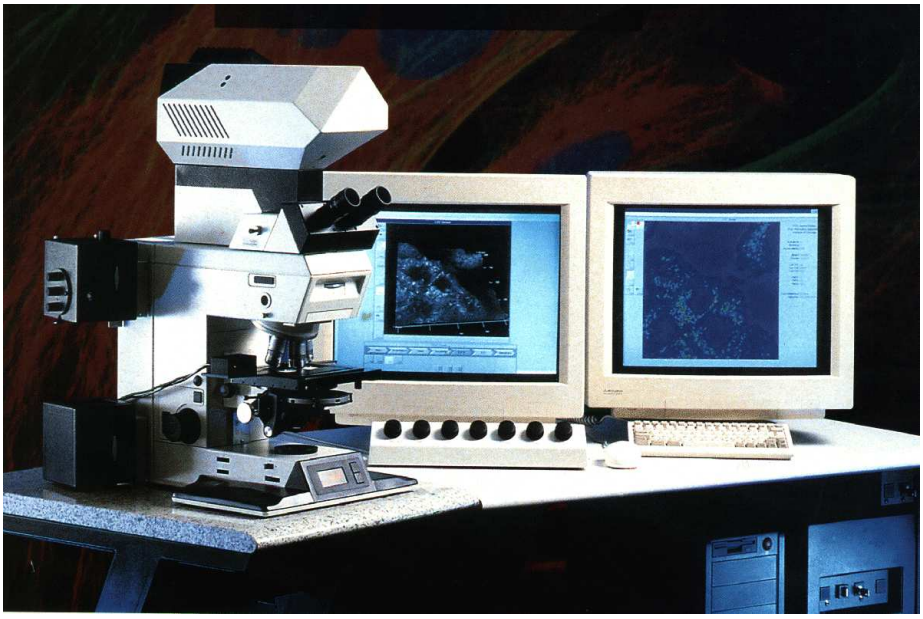

Fig. 3: confocal laser scanning microscope

Filtering Techniques

Due to the principle of the confocal laser-scanning microscope, artifacts like blurring and washed out edges must be removed from the data before creating an image from the data set.

Within a slice, the features of an object are rendered clearly with sharp edges, but across slices, down to a certain degree, the microscope delivers fuzzy information from neighboring slices, which interferes the image. This information must be detected and eliminated from the data before rendering.

For filtering, we are using a cubic matrix, which detects and elimates fuzzyness within a single slice as well as across adjoining slices. We use only 26 elements in the neighborhood, that is one element in each direction, including the diagonals.

We use the Laplacian operator for scalar fields (1):

$$\Delta V(P) = div\ grad\ V(P) \tag{1}$$

For a three-dimensional cartesian grid V at position $P = (x_0, y_0, z_0)$, we obtain:

$$\Delta V = \frac{\partial^2 V}{\partial x^2} + \frac{\partial^2 V}{\partial y^2} + \frac{\partial^2 V}{\partial z^2} \tag{2}$$

For a discrete version of (2), we can use the following mask (3):

$$\begin{aligned} K &= (K_1, K_2, K_3) \quad \text{with} \\ K_1 = K_3 &= \begin{pmatrix} 0 & 0 & 0 \\ 0 & -1 & 0 \\ 0 & 0 & 0 \end{pmatrix} \\ K_2 &= \begin{pmatrix} 0 & -1 & 0 \\ -1 & 6 & -1 \\ 0 & -1 & 0 \end{pmatrix} \end{aligned} \tag{3}$$

K_2 is meant to be aligned with the slice, while K_1 and K_3 refer to the neighboring slices.

As an improved version, which is less responsive to noise, we can also use (4):

$$\begin{aligned} L &= (L_1, L_2, L_3) \quad \text{with} \\ L_1 = L_3 &= \begin{pmatrix} 0 & 1 & 0 \\ 1 & -2 & 1 \\ 0 & 1 & 0 \end{pmatrix} \\ L_2 &= \begin{pmatrix} 1 & -2 & 1 \\ -2 & 2 & -2 \\ 1 & -2 & 1 \end{pmatrix} \end{aligned} \tag{4}$$

Since edge enhancement within a slice is not as important as feature enhancement and reduction of blurring across slices (5), we introduce a blending factor ω:

$$\begin{aligned} M &= (M_1, M_2, M_3) \quad \text{with} \\ M_1 = M_3 &= \begin{pmatrix} 0 & 1-\omega & 0 \\ 1-\omega & -2(1+\omega) & 1-\omega \\ 0 & 1-\omega & 0 \end{pmatrix} \\ M_2 &= \begin{pmatrix} 1-\omega & -2(1-\omega) & 1-\omega \\ -2(1-\omega) & 2(1+\omega) & -2(1-\omega) \\ 1-\omega & -2(1-\omega) & 1-\omega \end{pmatrix} \end{aligned} \tag{5}$$

For $\omega = 0$, M is identical to L; for $\omega = 1$, M detects features in z-direction only; for $\omega > 1$, the filtering effect across slices is enhanced. We found that for values of $\omega \in [0, \ldots, 5]$ we obtain good results.

Border pixels are handled by adding a periodical extension to the image in each direction [2]. The size of the filter matrix could be extended to more than 3 x 3 x 3, but for our application this would be unsuitable, because the smoothing effect would be exaggerated, and the influence on small features, which we are interested in, would be too strong.

Of course, before visualizing the filtered image, each pixel must be normalized using formula (6):

$$I'(P) = \frac{I(P)}{4(\omega + 1)} + \frac{1}{2} I_{\max} \qquad (6)$$

with $I_{\max}$ referring to the maximum pixel intensity.

Figure 4 shows a single slice from the original data set, while figure 5 shows the same slice with our filter matrix applied.

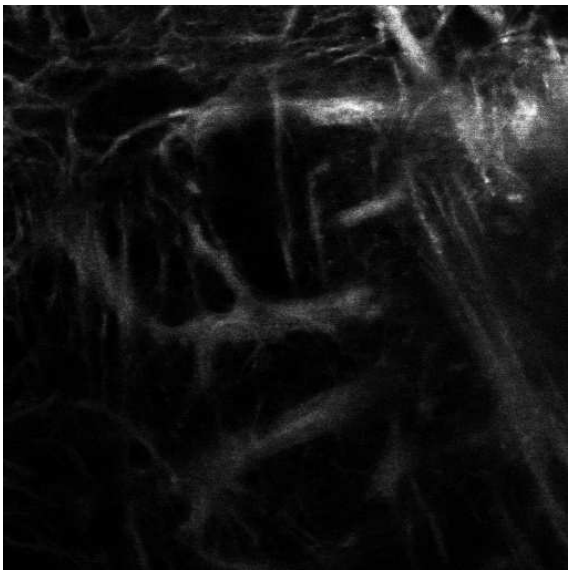

Fig. 4: original slice from a giant glial cell

Fig. 5: filtered image of glial cell (ω = 0.9)

A histogram equalization was applied to figure 5 before printing for better visibility.

Interactive Rendering

A giant glial cell within an isolated segmental ganglion of the leech was filled iontophoretically with the fluorescent dye Oregon Green BAPTA-1 (Molecular Probes, Eugene, OR, USA) and was monitored by a confocal laser-scanning microscope (Leica TCS 4D). A stack of 40 confocal images with a distance of 0.5 µm between the images was sampled.

The images were enhanced with our filtering method (see previous chapter), and fed into the rendering pipeline of our InVIS system [7]. InVIS was originally designed for medical applications (CT and MRI), but the addition of new features and filtering techniques enabled us to apply it also to biological data [6].

Different rendering algorithms, such as volume and surface rendering techniques, can be applied to a data set. For this application, we have selected an isosurface representation of the data set [4][8]. Figure 6 shows an example of a 3-D reconstruction of a glial cell from a leech *(Hirudo medicinalis).*

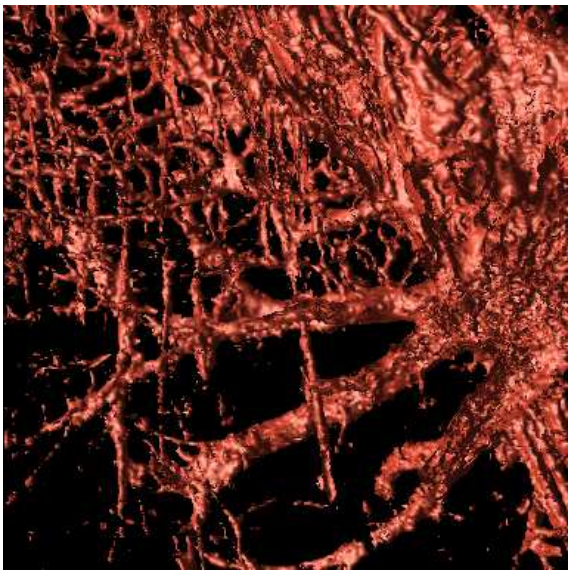

Fig. 6: 3-D reconstruction of a glial cell

Interactive visualization of large biological or medical data sets is a trade-off between quality and speed. Fast rendering can be achieved by data reduction, preprocessing of the data set, and a powerful graphics engine. Image quality is a significant factor, which must be considered for all stages of the rendering pipeline. For biological and medical applications, it is an important design factor that each stage preserves accuracy of data. If the algorithm is scalable, it should provide different levels of detail, which can be used to switch between different resolutions.

In our system, interactive control is implemented in each stage of the pipeline. A flexible import module allows us to read density (grey level) data as well as label data for segmentation at any resoultion and in any file or byte order. A *time control unit* (TCU) makes sure that during an animation the adaptive data reduction provides enough throughput to obtain an interactive behavior of the system [5]. The visibility transformation applies color and transparency to the object. Perspective and illumination are controlled by the GUI, which is implemented using an OpenGL interface to the graphics hardware. The system compiles platform-independently on UNIX workstations as well as on a regular PC platform (figure 7).

The system was tested on SGI Indigo 2 High Impact (R4400, IRIX 5.3), SGI Indy (R5000, IRIX 6.2), HP 400 (M68040, HP-UX 8.0), and PC (Intel Pentium 133 MHz, MS-Windows 95/NT4.0) platforms. The portable design of the user interface required no platform-specific changes.

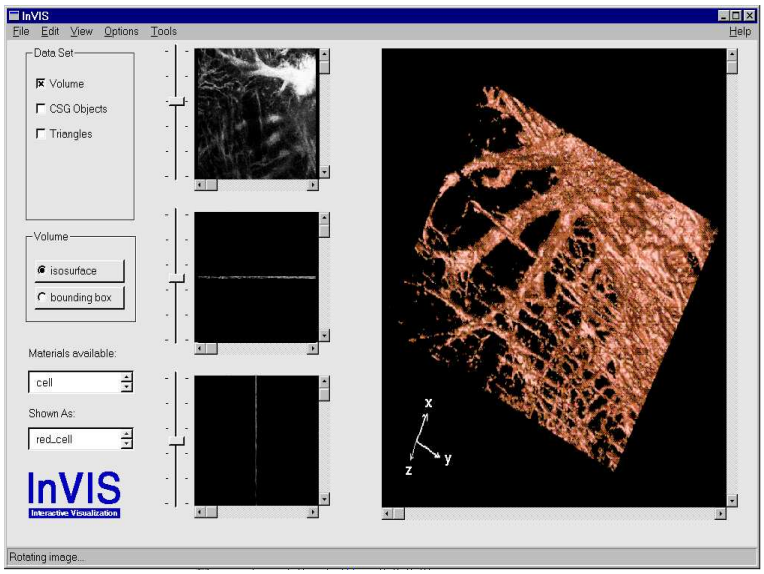

Fig. 7: InVIS user interface

Conclusions

We have introduced a method to navigate interactively through a virtual data set from a confocal laser-scanning microscope. The image series consists of a set of slices, similar to other imaging techniques, such as CT and MRI.

Therefore, we have applied our rendering system, which was originally designed for medical data, to a biological data sets. Special filtering techniques were incorporated to enhance the visualization of the data set.

We found that interactive navigation through the data set provides more information than the regular view through the microscope, which can only browse through the slices. The perception of nested structures within the cell is easier with our system. The performance of a standard PC satisfies the requirements for interactive manipulation of the data set.

References

[1] R. E. Coggeshall and D. W. Fawcett. The fine structure of the central nervous system of the leech Hirudo medicinalis. *J. Neurophysiol.*, 27:229 – 289, 1964.

[2] P. Haberäcker. *Digitale Bildverarbeitung: Grundlagen und Anwendungen*. Hanser-Studienbücher, München, Wien, 1987.

[3] C. Lohr and J. W. Deitmer. Structural and physiological properties of leech giant glial cells as studied by confocal microscopy. *Exp. Biol. Online*, 2:8, 1997.

[4] W. E. Lorensen and H. E. Cline. Marching Cubes: A high resoultion 3D surface construction algorithm. *ACM Proceedings, Computer Graphics*, 21(4):163 – 169, 1987.

[5] J. Meyer, S. Gelder, C. Heiming, and H. Hagen. Interactive Rendering – A Time-Based Approach. *SIAM Conference on Geometric Design '97, Nashville, Tennessee*, p. 23, 1997.

[6] J. Meyer, S. Gelder, K. Kretschmer, K. Silkenbäumer, and H. Hagen. Interactive visualization of hybrid medical data sets. *Proc. of WSCG '97, Pilsen, Czech Republic*, 2:371 – 380, 1997.

[7] J. Meyer, S. Gelder, T. E. Schneider, and H. Hagen. InVIS – Interactive visualization of medical data sets. *Proc. of Scientific Visualization '97, Schloß Dagstuhl, Germany*, 1997

[8] C. Montani, R. Scateni, and R. Scopigno. A modified look-up table for implicit disambiguation of Marching Cubes. *The Visual Computer*, 10:353 – 355, 1994.

[9] C. R. Rose and J. W. Deitmer. Evidence that glial cells modulate extracellular pH transients induced by neuronal activity in the leech central nervous system. *J. Physiol.*, 481:1 – 5, 1994.

[10] C. R. Rose, C. Lohr, and J. W. Deitmer. Activity-induced Ca^{2+} transients in nerve and glial cells in the leech CNS. *NeuroReport*, 6:642 – 644, 1995.

[11] A. Vernadakis. Glia-neuron intercommunications and synaptic plasticity. *Prog. Neurobiol.*, 49:185 – 214, 1996.